

PAPER • OPEN ACCESS

## Polarization reconstruction algorithm for a Compton polarimeter

To cite this article: M Vockert *et al* 2018 *J. Phys.: Conf. Ser.* **1024** 012041

View the [article online](#) for updates and enhancements.

### Related content

- [Identification and reduction of unwanted stray radiation using an energy- and position-sensitive Compton polarimeter](#)  
K-H Blumenhagen, U Spillmann, T Gaßner et al.
- [Employing digital pulse processing electronics for the readout of a Si\(Li\)-Compton-polarimeter for the SPARC collaboration](#)  
U Spillmann, K H Blumenhagen, E Badura et al.
- [Polarization studies of radiative electron capture into highly-charged uranium ions](#)  
S Hess, H Bräuning, U Spillmann et al.



**IOP | ebooks™**

Bringing you innovative digital publishing with leading voices to create your essential collection of books in STEM research.

Start exploring the collection - download the first chapter of every title for free.

# Polarization reconstruction algorithm for a Compton polarimeter

M Vockert<sup>1,2</sup>, G Weber<sup>2</sup>, U Spillmann<sup>3</sup>, T Krings<sup>4</sup> and Th Stöhlker<sup>1,2,3</sup>

<sup>1</sup> Institute for Optics and Quantum Electronics, Friedrich Schiller University Jena, Max-Wien-Platz 1, 07743 Jena, Germany

<sup>2</sup> Helmholtz Institute Jena, Fröbelstieg 3, 07743 Jena, Germany

<sup>3</sup> GSI Helmholtzzentrum für Schwerionenforschung GmbH, Planckstraße 1, 64291 Darmstadt, Germany

<sup>4</sup> Institut für Kernphysik, Forschungszentrum Jülich, Wilhelm-Johnen-Straße, 52425 Jülich, Germany

E-mail: [Marco.Vockert@uni-jena.de](mailto:Marco.Vockert@uni-jena.de)

**Abstract.** We present the technique of Compton polarimetry using X-ray detectors based on double-sided segmented semiconductor crystals that were developed within the SPARC collaboration. In addition, we discuss the polarization reconstruction algorithm with particular emphasis on systematic deviations between the observed detector response and our model function for the Compton scattering distribution inside the detector.

## 1. Introduction

The study of particle and photon polarization phenomena occurring in the interaction of fast ion and electron beams with matter is of particular relevance for the understanding of cosmic and laboratory plasmas, where high temperatures, high atomic charge states and high field strengths prevail. In addition, polarization-sensitive studies of radiation emitted by processes in highly-charged, heavy ions may provide detailed insights into both relativistic particle dynamics and atomic structure properties at extreme electromagnetic field strengths [1, 2]. In recent years, polarimetry of hard X-rays was also proven to be a unique tool to study subtle spin-dependent effects in the realm of atomic physics at high field strengths [3, 4]. With high-precision X-ray polarimetry even quantum electrodynamic and parity nonconservation effects may become accessible [5, 6]. Moreover, X-ray polarimetry is proposed as a tool for the diagnosis of spin-polarized ion beams for future experiments at the Facility for Antiproton and Ion Research (FAIR) [7].

A significant part of the recent hard X-ray polarization measurements were performed within the Stored Particle Atomic Research Collaboration (SPARC) [8] using polarimeters based on double-sided segmented semiconductor crystals. These devices employ a detector technology that has been continuously improved over the last two decades [9, 10, 11]. In this report we will briefly present the technique of polarization measurements with such detectors and then focus on the present status of the analysis of possible systematic uncertainties introduced by our reconstruction method for the incident X-ray (linear) polarization.



## 2. Compton polarimetry

The angular differential cross section of the Compton scattering process is described by the Klein-Nishina equation (Eq. 1):

$$\frac{d\sigma}{d\Omega} = \frac{1}{2}r_0^2 \left(\frac{E'}{E}\right)^2 \left(\frac{E'}{E} + \frac{E}{E'} - 2\sin^2\theta \cos^2\varphi\right) \quad (1)$$

where  $E$  denotes the incident photon energy and  $E'(\theta)$  the photon energy after the scattering with the corresponding polar scattering angle  $\theta$ , while  $\varphi$  is the azimuthal scattering angle and  $r_0$  being the classical electron radius. Note that the scattered photon is preferably emitted perpendicular to the incident photon electric field vector, whereas emission in the parallel direction is less probable. Thus, the degree of linear polarization as well as the orientation of the polarization axis of an incident photon beam can be obtained from the azimuthal emission pattern of Compton scattered photons. A detailed discussion of this technique can be found in Ref. [12].

Within the SPARC collaboration several double-sided segmented X-ray detectors were constructed as dedicated Compton polarimeters [10, 11, 13]. They provide good detection efficiency, energy and time resolution together with millimeter to submillimeter two-dimensional position resolution and a large detection area. When an incident photon undergoes Compton scattering inside such a detector, the scattered photon may be detected at a different position within the same detector crystal. Thus each segment of the detector crystal serves as both a scatterer and an absorber for the scattered X-rays, resulting in a high polarimeter efficiency due to a large active area and a good coverage of the azimuthal scattering angle. Combining energy, position and time information of each interaction then allows a reconstruction of the Compton scattering events [14]. A series of recent measurements demonstrated the detector ability for precise and efficient linear polarization studies [4, 15, 16, 17]. Depending on the crystal material and thickness, which can reach up to about 2 cm, polarimeters of the aforementioned type can be tailored to incident photon energies ranging from a few dozen keV up to the MeV regime.

In the following we will focus on data associated with a recently commissioned Si(Li) Compton polarimeter (Fig. 1 a). This instrument consists of a 9 mm thick lithium-drifted silicon crystal,

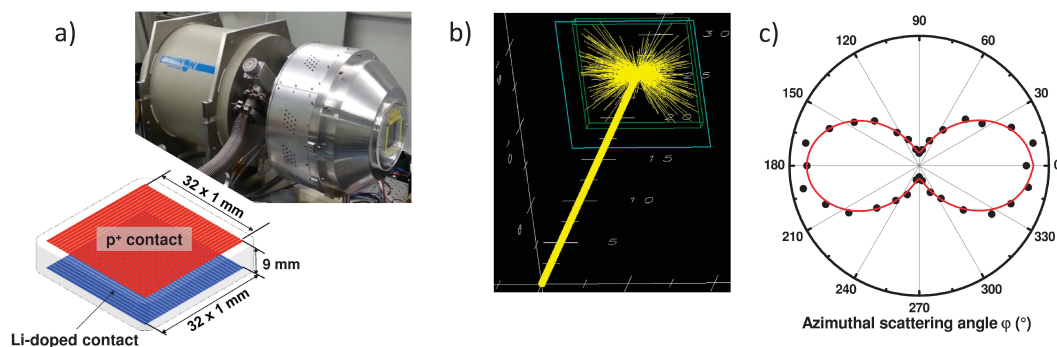


**Figure 1.** a) Photograph of a recently commissioned Compton polarimeter developed within the SPARC collaboration, together with a schematic drawing of the double-sided segmented detector crystal. b) MC simulation of Compton scattering of a 100% polarized photon beam impinging on the detector crystal. c) Azimuthal scattering distribution for highly polarized K-REC photons generated at the ESR storage ring [13] (black dots) plotted together with the model curve (red line) shown in Eq. 2, being adjusted to the experimental data.

segmented on each side into 32 strips of 1 mm width each, and features an improved energy

resolution compared to polarimeters developed previously, see [13] for details. The Monte Carlo (MC-)simulated scattering distribution of a 100% polarized beam impinging on the detector crystal is illustrated in Fig. 1 b), exhibiting a pronounced anisotropy as expected from Eq. 1. Finally, Fig. 1 c) displays the azimuthal scattering distribution of nearly 100% polarized X-ray radiation recorded in a commissioning experiment of the aforementioned Si(Li) polarimeter. These photons result from radiative electron capture (REC) into the projectile K shell (K-REC) during the collision of bare xenon ions at an energy of 30.93 MeV/u with hydrogen molecules at the internal gas target of the experimental storage ring (ESR) of the GSI facility at Darmstadt, Germany [18], and are known to exhibit a high degree of linear polarization [19, 20]. To extract the degree of linear polarization, a model function based on the Klein-Nishina equation is adjusted to the experimental data. This function is of the form

$$f(\varphi) = C \left( A - 2B \left( \frac{1}{2}(1 - \widetilde{P}_L) + \widetilde{P}_L \cos^2(\varphi + \varphi_0) \right) \right). \quad (2)$$

Therein the parameters  $A$ ,  $B$  and the normalizing factor  $C$  are defined as:

$$A = \frac{1}{I} \sum_{\theta=\theta_0}^{\theta_1} I_{\theta} \left( \frac{E'(\theta)}{E} + \frac{E}{E'(\theta)} \right) \quad ; \quad B = \frac{1}{I} \sum_{\theta=\theta_0}^{\theta_1} I_{\theta} \sin^2 \theta \quad ; \quad C = \frac{I}{N_B} \frac{1}{A - B}$$

wherein  $I_{\theta}$  is the number of acquired Compton events at the scattering angle  $\theta$  (being already corrected for geometric effects due to the angular binning and finite position resolution of the detector),  $I$  is the sum of all reconstructed Compton events over the interval  $[\theta_0, \theta_1]$  (usually selected as  $(90 \pm 15)^\circ$  [11]) and  $N_B$  is the number of angular bins. The energies  $E$  and  $E'(\theta)$  are defined as in Eq. 1. The reconstructed degree of linear polarization  $\widetilde{P}_L$  and the orientation of the polarization vector with respect to the detector axis  $\varphi_0$  are free parameters that are adjusted to the experimental data by means of a least-squares optimization. Note that the degree of linear polarization of the incident radiation is obtained from  $\widetilde{P}_L$  after correcting for the polarimeter quality and other effects as explained in Ref. [14]. However, this is beyond the scope of the present work.

### 3. Systematic deviation of detector response function and model function

When drawing conclusions from the output of the reconstruction algorithm, it is crucial to quantify to what extent the model reproduces the real detector response to incident polarized X-rays. This is of particular importance for precision experiments aiming for an accuracy of better than 1% in the determination of the degree of polarization. In order to determine the level of statistical uncertainty below which systematic deviations between the detector response and our model function emerge as the dominant contribution to the overall uncertainty of the reconstructed polarization characteristics, we performed a series of MC simulations based on the EGS5 (Electron-Gamma Shower) package [21]. It was previously found that such simulations are able to reproduce all relevant detector features encountered in real-world measurements [14, 22]. As a test case we used the experimental setup and incident radiation characteristics of the recent commissioning measurement for the new Si(Li) polarimeter. From the measured data we obtained a preliminary value of the degree of linear polarization of  $(0.860 \pm 0.008)$ , based on about 17 000 reconstructed Compton events (without applying any corrections to account for polarimeter quality, misidentified Compton events, etc.). With our simulation routine we replicated the experimental conditions and used incident REC radiation data obtained from the REC calculator (RECAL) code [23, 24] to produce data sets with the number of reconstructed Compton events ranging from  $10^3$  to  $10^6$ . Two of these data sets, illustrating the difference between low and high numbers of reconstructed Compton events, are presented in Fig. 2. Here

the azimuthal scattering distribution is plotted for the simulated data together with the model function, shown in Eq. 2, which using the degree of linear polarization as a free parameter models these data sets. A significant deviation between the data set and our model is indicated

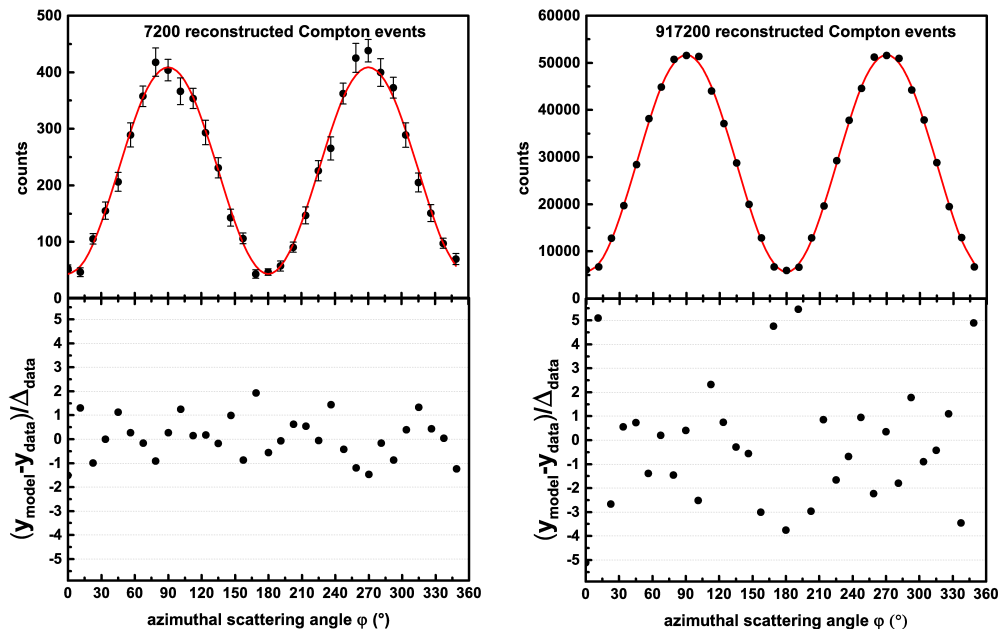


**Figure 2.** Top pair: Azimuthal scattering distribution (black dots) including error bars indicating the  $1\sigma$  statistical uncertainty, together with fitted curve using Eq. 2 (red line) for low (left) and very high statistics (right). Bottom pair: Difference between obtained data points and the fitted curve, relative to the individual errors, for data sets with low (left) and very high statistics (right).

by a high number of data points deviating more than the standard deviation (being determined by the statistical uncertainty of the data) from the model. A systematic deviation is clearly found for the ‘high statistics’ data set shown on the right side of Fig. 2. To quantify this deviation for a whole data set we used the reduced chi-squared  $\chi_{\text{red}}^2 = \frac{\chi^2}{N}$  ( $\chi^2$  being the weighted sum of the squared difference between the data points and the associated fitted curve and  $N$  being the number of data points minus the number of free parameters), which is plotted as a function of the number of reconstructed Compton events in Fig. 3. As a rule of thumb, a  $\chi_{\text{red}}^2$  value  $\gg 1$  indicates a model that does not capture all significant features of a given data set. This is the case for the data sets consisting more than about 30 000 reconstructed Compton events. In this region the use of Eq. 2 to reconstruct the polarization of the incident radiation is questionable as the  $\chi_{\text{red}}^2$  is rapidly increasing with decreasing statistical uncertainty of the data. Nonetheless, the amount of data obtained in our commissioning experiment is in the range of about 17 000 reconstructed Compton events and therefore still well within the reliability range of our model. The reconstructed degree of linear polarization is also presented in Fig. 3, with error bars corresponding to the statistical uncertainty. It is found that, while all polarization values are in agreement with each other, there is a slight trend towards lower polarization values with decreasing statistical uncertainty. This hints at the presence of a systematic effect that becomes significant once the statistical uncertainty drops below a certain level.

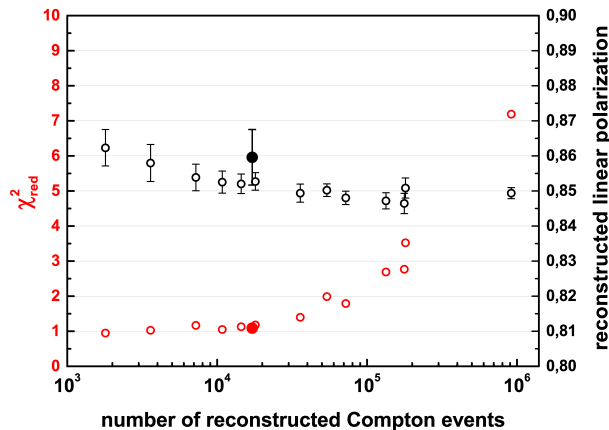


**Figure 3.** Values of the reduced chi-squared  $\chi_{\text{red}}^2$  (red circles) and reconstructed linear polarization (black circles) for multiple simulated data sets with different statistical uncertainties. In addition, points in the plot are displayed for comparison with experimental data points (filled dots), taken from the commissioning experiment at ESR [13].

#### 4. Summary

The current status of our analysis indicates that our simple model based on the Klein-Nishina equation apparently works for small statistics, but the equation is not able to describe fully the azimuthal scattering distribution of reconstructed Compton events at high statistics. To further improve our analysis and understanding of the data, studies on higher statistics are ongoing and alternative reconstruction algorithms are taken into account.

#### References

- [1] Stöhlker Th et al. 2009 *Eur. Phys. J.-Spec. Top.* **169** 5–14
- [2] Weber G et al. 2015 *J. Phys. Conf. Ser.* **583** 012041
- [3] Tashenov S et al. 2011 *Phys. Rev. Lett.* **107** 173201
- [4] Martin R et al. 2012 *Phys. Rev. Lett.* **108** 264801
- [5] Marx B et al. 2013 *Phys. Rev. Lett.* **110** 254801
- [6] Fratini F, Trotsenko S, Tashenov S, Stöhlker Th and Surzhykov A 2011 *Phys. Rev. A* **83** 052505
- [7] Surzhykov A, Fritzsche S, Stöhlker Th and Tashenov S 2005 *Phys. Rev. Lett.* **94** 203202
- [8] Stöhlker Th et al. 2011 *AIP Conf. Proc.* **1336** 132–7
- [9] Kroeger R A, Johnson W N, Kurfess J D and Philips B F 1999 *Nucl. Instrum. Meth. A* **436** 165–9
- [10] Spillmann U et al. 2008 *Rev. Sci. Instrum.* **79** 083101
- [11] Weber G et al. 2010 *J. Instrum.* **5** C07010
- [12] Lei F, Dean A J and Hills G L 1997 *Space Sci. Rev.* **82** 309–88
- [13] Vockert M et al. 2017 *Nucl. Instrum. Meth. B* **408** 313–6
- [14] Weber G et al. 2015 *J. Phys. B* **48** 144031
- [15] Weber G et al. 2010 *Phys. Rev. Lett.* **105** 243002
- [16] Blumenhagen K H et al. 2016 *New J. Phys.* **18** 103034
- [17] Hess S et al. 2009 *J. Phys. Conf. Ser.* **163** 012072
- [18] Vockert M et al. to be published 2017
- [19] Hess S et al. 2009 *J. Phys. Conf. Ser.* **194** 012025
- [20] Tashenov S et al. 2006 *Phys. Rev. Lett.* **97** 223202
- [21] Hirayama H, Namito Y, Bielajew A F, Wildermann S J and Nelson W R 2005 *SLAC report* SLAC-R-730
- [22] Weber G, Bräuning H, Martin R, Spillmann U and Stöhlker Th 2011 *Phys. Scripta* **T144** 014034
- [23] Weber G, Ding H, Herdrich M O and Surzhykov A 2015 *J. Phys. Conf. Ser.* **599** 012040
- [24] Herdrich M O, Weber G, Gumberidze A, Wu Z W and Stöhlker Th 2017 *Nucl. Instrum. Meth. B* **408** 294–300